Charge-Based Supercapacitor Storage Estimation for Indoor Sub-mW Photovoltaic Energy Harvesting Powered Wireless Sensor Nodes

Xicai Yue, *Senior Member, IEEE*, Janice Kiely, Des Gibson, and Emmanuel M. Drakakis, *Member, IEEE*

***Abstract*—Supercapacitors offer an attractive energy storage solution for lifetime "fit and forget" photovoltaic (PV) energy harvesting powered wireless sensor nodes for Internet of Things (IoT) applications. Whilst their low storage capacity is not an issue for sub-mW PV applications, energy loss in the charge redistribution process is a concern. Currently, there is no effective method to estimate the storage of the supercapacitor in IoT applications for optimal performance with sub-mW input. The existing energy-based method requires supercapacitor model parameters to be obtained and the initial charge state to be determined, consequently it is not suitable for practical applications. This paper defines a charge-based method, which can directly evaluate supercapacitor's storage with straightforward calculations. Time constant analysis and experimental tests demonstrate that with the newly proposed method, the manufacturer-specified tiny leakage current, although measured long after postcharge (e.g., 72 h), can be directly used, making the storage estimation for a supercapacitor in IoT applications as simple as that for an ordinary capacitor. In addition, the demonstrated tiny leakage current at the required energy storage for a sub-mW PV-powered IoT application enables a supercapacitor alone to be employed as the storage mechanism, thus achieving lifetime battery-replacement-free, self-powered IoT nodes.**

***Index Terms*—Charge analysis, charge redistribution, current-mode circuit analysis, energy harvesting, Internet of Things (IoT), leakage current, photovoltaic (PV), self-discharge, supercapacitor.**

Manuscript received May 1, 2018; revised September 26, 2018 and December 5, 2018; accepted January 3, 2019. Date of publication March 25, 2019; date of current version October 31, 2019. This work was supported by the Innovate U.K. under Contract 102156. *(Corresponding author: Xicai Yue.)*

X. Yue is with the Faculty of Environment and Technology, Department of Engineering Design and Mathematics, University of the West of England, BS16 1QY Bristol, U.K. (e-mail: alex.yue@uwe.ac.uk).

J. Kiely is with the Institute of Bio-Sensing Technology, University of the West of England, BS16 1QY Bristol, U.K. (e-mail: janice.kiely@uwe.ac.uk).

D. Gibson is with the Gas Sensing Solutions, Glasgow G68 9HQ, U.K., and also with the Institute of Thin Films, Sensors and Imaging, University of the West of Scotland, Scottish Universities Physics Alliance, PA1 2BE Paisley, U.K. (e-mail: des.gibson@uws.ac.uk).

E. M. Drakakis is with the Department of Bioengineering, Imperial College London, SW7 2AZ London, U.K. (e-mail: e.drakakis@imperial.ac.uk).

Color versions of one or more of the figures in this paper are available online at http://ieeexplore.ieee.org.

Digital Object Identifier 10.1109/TIE.2019.2896321

I. Introduction

PHOTOVOLTAIC (PV) energy harvesting provides a potential solution for "fit and forget" self-powered autonomous nodes used in wireless sensor networks (WSN)/Internet of Things (IoT) applications, making it unnecessary to replace the battery over the product lifetime. It is estimated that there will be 45 billion WSN/IoT nodes existing in the world by 2020 [1]; therefore, a maintenance-free energy harvesting solution will soon become a very attractive solution, since environmental and economic costs of replacing and maintaining batteries will be excessive.

For indoor IoT applications, such as smart buildings or independent living, environmental or physiological parameters often change slowly, so sensors located in the IoT nodes need to measure in minutes/hours/days rather than continuously. The power that an ambient energy harvester can produce might be lower than that required for an individual measurement, but the harvested energy can be continuously accumulated into energy storage components [such as a Lithium (Li) battery or a supercapacitor] so that a high-power pulse can be supplied for a short-term measurement.

The power density of indoor PV energy harvesting devices (10–20 μW/cm^2) is much higher than that of RF (0. 1 μW/cm^2 for GSM, 0.001 μW/cm^2 for WiFi), making PVs the most suitable for indoor IoT applications. However, when considering that the energy harvested from a credit card size (85 $\times$ 55 mm) indoor PV panel is lower than 0.8 mW, either a Li-battery or a supercapacitor must be used in conjunction with the sub-mW indoor PV energy harvester to provide the required storage capacity.

The total number of recharge cycles for the lifetime of a Li-battery is several hundreds. Although a Li-battery/supercapacitor hybrid storage system can extend the battery lifetime, to some extent, by reducing battery peak discharge current, there is no guarantee that the requirements for lifetime "fit and forget" applications can be fully met when considering

the limit on the number of recharge-cycles. By contrast, a supercapacitor can withstand millions of charge cycles (corresponding to an estimated 20 years lifetime [2], [3]), giving it a significant advantage as an energy storage solution for lifetime "fit and forget" IoT applications.

The energy loss caused by self-discharge of a supercapacitor [4] is a concern when using a supercapacitor alone, especially in sub-mW energy harvesting powered IoT applications. A method to calculate the storage energy loss during the charge redistribution process for energy-sensitive IoT applications has been identified [4]. It requires the use of a supercapacitor model, which is usually not directly available from the manufacturer, so further measurements are required to obtain the model parameters [5], [6] and, most importantly, it requires the charge state of the supercapacitor (the initial conditions of the energy storage calculation [7]–[9]) to be known, making the method impractical. On the other hand, given that the storage of the supercapacitor can be evaluated via either the energy ($\frac{1}{2}CV^2$) or the charge (CV), a charge-based storage evaluation method may simplify the supercapacitor's storage evaluation for PV-powered IoTs.

It has been reported that the self-discharge of the supercapacitor changes with time and is relatively high in the first hours after charging [10]. However, the available self-discharge related parameters provided by the manufacturer, such as the leakage current, is measured a relatively long time after charging, for example, 2.0 μA leakage after 72 h postcharging for the 5.4V 0.5F supercapacitor from VinaTech. In IoT applications, the storage supercapacitor is repeatedly charged and discharged in every measurement period, which is highly unlikely to be longer than 72 h.

The self-discharge current of the supercapacitor in an indoor PV energy harvesting application has been reported as being as high as a half of the average load current [11]. It has also been concluded that "using a supercapacitor alone as a long-term storage solution is unfeasible for sub-mW indoor PV energy harvesting applications" due to the high self-discharge rate of the supercapacitor [12]. Nevertheless, for a PV energy harvesting powered IoT node with supercapacitor storage, tested under solar irradiance of 100–440 W/m^2 [13] (corresponding to tens of mA PV current), the μA self-discharge level of the supercapacitor was of no concern. However, for indoor applications when the illumination conditions are set as 200 lx (0.3 W/m^2), a PV of the same size will produce a current in tens of μA, making it impossible to ignore the μA leakage current level of the supercapacitor. Recently, an indoor PV energy harvested IoT node using a supercapacitor alone as storage has been presented [14], which demonstrated that the dynamic leakage current of the supercapacitor is low for this application. This finding has been supported by a recent paper estimating the dynamic leakage current of supercapacitor in an IoT sensor node [15]. Therefore, if the leakage current of a supercapacitor is as low as reported, there is a possibility to use a supercapacitor alone as the storage in sub-mW indoor PV energy harvesting applications to provide a lifetime, battery replacement-free, solution.

This paper proposes a novel charge-based supercapacitor storage evaluation method to calculate the available storage in indoor PV energy harvesting powered IoT applications. This work was carried out during an Innovate UK project, looking at smart air quality control in buildings using autonomous IoT nodes with a supercapacitor as the sole energy storage component. Section II describes the proposed charge-based storage evaluation method to be used when the power management strategy is focused on maintaining charge stored in the supercapacitor in order to ensure that the total charge to the supercapacitor is not smaller than the total discharge. Section III details the validation experiments demonstrating that the leakage current of the supercapacitor in an IoT application is the same as that of the manufacturer-specified value, so the charge stored in the supercapacitor can be directly calculated based on the newly proposed method. Finally, Section IV concludes this paper.

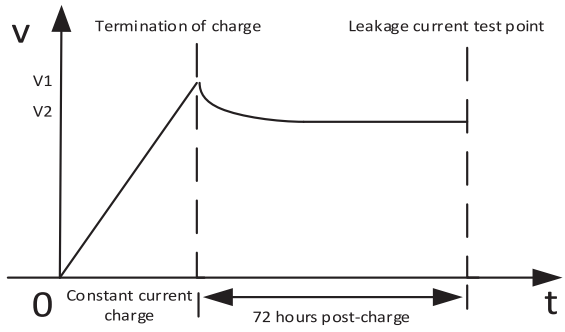

Fig. 1. Self-discharge of the supercapacitor.

II. Charge-Based Storage Evaluation for a Supercapacitor

A. Charge Redistribution Caused Energy Loss

The capacitance $C(t)$ of a supercapacitor is typically modeled by a leakage path of R_{leak} and a number of parallel RC branches [15]. The time constant (τ) to fully charge a supercapacitor is expressed as $\tau = \sum_{i=0}^{n} (C_i \times \sum_{j=0}^{i} R_j)$, where C_0 represents the capacitance formed near the electrodes and a larger n represents the equivalent components in a deeper branch.

Fig. 1 shows the charge/self-discharge profile of a supercapacitor, demonstrates that the supercapacitor is charged by a constant current to V_1 and then the terminal voltage of the supercapacitor exponentially drops to V_2, caused by the charge redistribution process. This charge redistribution process transfers charge to deeper branches, making the capacitance of a postcharge supercapacitor increase with time to reach its nominal value at the end of the charge redistribution process. This is because at the end of the charge redistribution process, the current flow through the internal resistor R_n is almost zero, making all the capacitors in the charge branches virtually be in parallel.

In IoT applications, the charge/discharge period, which is the entire measurement period including the active measurement phase and the sleep phase, is much shorter than 72 h. As a result, the supercapacitor stays in the beginning of the charge redistribution process for each measurement period where the exponentially reducing terminal voltage corresponds to an

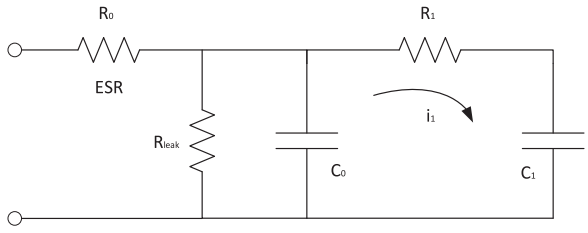

Fig. 2. Two-stage supercapacitor model for energy loss estimation.

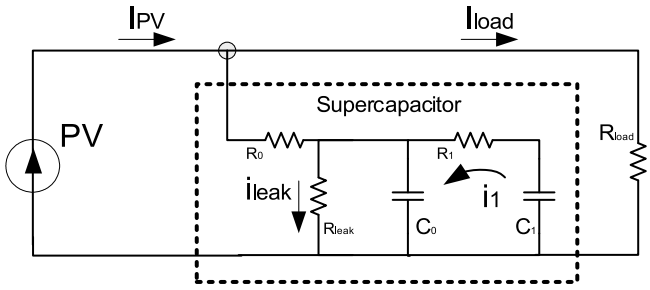

Fig. 3. Charge-based storage estimation for supercapacitor in IoTs.

exponentially varying current. When this current flows through the internal resistance of R_n, it causes stored energy loss. A simplified two-stage supercapacitor model, as shown in Fig. 2, which accurately simulates several hours postcharge behavior of the supercapacitor [9], [16]–[18], has been used for storage estimation in an IoT process [4], where energy loss in the charge redistribution process can be calculated as $\int_0^{t_0} i_1^2(t) R_1 dt$. However, this method is difficult to implement since the model parameters of a commercially available supercapacitor are unknown and the initial charge conditions are different from one application to another.

B. Charge-Based Supercapacitor Storage Estimation

When a supercapacitor is used as the energy storage in IoT applications, the supercapacitor is repeatedly charged in sleep mode (denoted as T_1) and discharged in active mode (denoted as T_2) of every measurement period $T = T_1 + T_2$. The amount of charge stored in a supercapacitor can be calculated using the capacitance multiplied by the terminal voltage ($C \times V$), whereas the amount of the charge change can be calculated using the charge/discharge current multiplied by the charge/discharge time ($I \times t$). When the energy harvested is larger than that consumed in the period T, the supercapacitor has a net charge, so an unremitting terminal voltage increase can be observed for each period, otherwise the net discharge results in a decrease in terminal voltage.

To evaluate the amount of charge stored in the supercapacitor, the indoor PV energy harvesting powered IoT node is analyzed in current mode, as shown in Fig. 3. The amount of charge change (ΔQ) of the supercapacitor in an entire measurement period can be written as

$$\Delta Q = (I_{\text{pv}} - I_{\text{leak}} - I_{\text{load}}) \times T \tag{1}$$

where

$$I_{\text{load}} = \frac{I_{\text{sleep}} \times T_1 + I_{\text{active}} \times T_2}{T}.$$

In sub-mW indoor PV-powered IoT applications, the μA PV charge current in sleep mode does not cause an observable charge redistribution process, i.e., charge transfer between C_0 and C_1. The tens of mA discharge current in active mode incur charge redistribution, a process that starts at the end of active mode; in view of this, the direction of the charge redistribution current of i_1 shown in Fig. 3 is not the same as that shown in Fig. 2 where the charge redistribution process happens after charge. The charge reduction from C_1 at time t_0 of the charge redistribution process is $\int_0^{t_0} i_1(t)dt$, which is the same as the charge increased in C_0, since the current to discharge the capacitor C_1 is the same as that to charge C_0. Therefore, the total amount of charge stored does not vary. For charge redistribution, only the leakage path of R_{leak} in Fig. 3 should be considered in a charge-based storage evaluation; no other calculations are required.

Using formula (1) to calculate the charge stored in the supercapacitor for an IoT application seems straightforward: I_{load} is a known parameter for a specific application and I_{pv} is a known parameter for a given illumination condition. However, the manufacturer-provided I_{leak}, a long time postcharge, is measured and thus intuitively it seems hard to evaluate how this parameter can be directly used to calculate the charge stored in the supercapacitor, where it is charged/discharged in the much shorter measurement period.

The charge redistribution induced current i_1 (t) shown in Fig. 3 can be expressed as

$$V_0 - \frac{1}{C_0}\int i_1(t)\,dt - \left(V_1 - \frac{1}{C_1}\int i_1(t)\,dt\right) = i_1(t)\,R_1$$

$$i_1(t) = \frac{V_0 - V_1}{R_1} e^{-\frac{t}{R_1 C_2}}, C_2 = \frac{C_0 C_1}{C_0 + C_1} \tag{2}$$

where V_0 and V_1 denote the voltages across capacitor C_0 and C_1 after charge which are charge history related ($V_0 < V_1$). When $t >> \tau = R_1 C_2$, charge redistribution is completed resulting in i_1 (t) $\simeq 0$ and accordingly it holds

$$V_0 = V_1, C = \frac{C_0 V_0 + C_1 V_1}{V_0} = C_0 + C_1 \tag{3}$$

therefore, it is possible to obtain the leakage current of the supercapacitor via terminal voltage and the nominated capacitance C using $I_{\text{leak}} = \text{C} \times \Delta\text{V}/\Delta\text{t}$, where $\Delta t = t_2 - t_1$ and $t_1, t_2 >> \tau$ to ensure the capacitance of the supercapacitor is the nominated one.

To demonstrate that the time constant of the charge redistribution is much smaller than the 72 h (typical leakage current measurement time after charge [10]), the parameters of the supercapacitor models from the literature are listed in Table I. The calculated time constants for charge redistribution of the supercapacitor are within 10 min and therefore, when leakage current is measured by the manufacturer, no leakage current from the charge redistribution process is included in the measurement,

TABLE I
TIME CONSTANT FOR CHARGE REDISTRIBUTION OF DIFFERENT SUPERCAPACITORS

	R_0 (Ω)	C_0 (F)	R_1 (Ω)	C_1 (F)	τ (s)
Ref [4]	66.7m	7.28	140	1.91	211.8
Ref [10]	48.3m	8.48	100	3.44	244.7
Ref [11]	0.46m	1.78K	1.98	0.18K	323.6

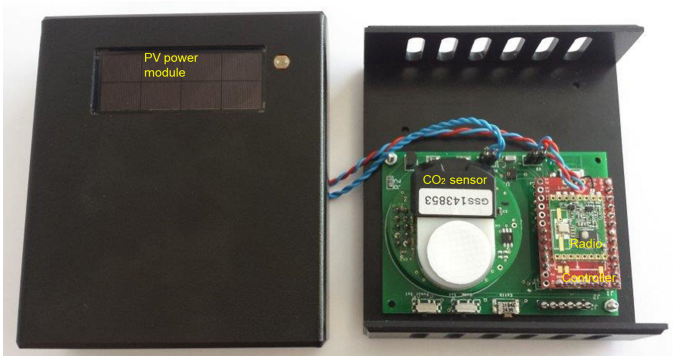

Fig. 4. Developed 70 × 50 × 20 mm autonomous IoT node for building ventilation. Left-hand side image: the window area is the mounted PV energy harvesting power supply. Right-hand side image: the sensor mounted can be seen on the left hand-side, and the microcontroller (red board) on the right. The green radio board sits on top of the microcontroller.

due to the condition of $t >> \tau$ (72 hours is hundreds times larger than the time constant of charge redistribution). Therefore, the manufacturer-provided leakage figure is the I_{leak} value shown in Fig. 3 and in formula (1).

It is concluded that although the time duration of the charge redistribution process depends on the charge history (amount of charge, initial charge condition, etc.), the charge redistribution process terminates far earlier than the end of the sleep period in sub-mW powered IoT applications [15]. This makes formula (1) a powerful tool for optimizing the PV powering system using $\Delta Q = C\Delta V$ at the end of sleep mode where C is the nominal value of the supercapacitor. Knowing the leakage current of the supercapacitor, the minimum measurement period at a given illumination $T_{\min}$ can be calculated by setting $\Delta Q = 0$ (can be inferred by $\Delta V = 0$) in formula (1). Similarly, the minimum PV panel area can be calculated for a given measurement period, since the maximum total discharge (discharge for a measurement plus discharge in sleep mode) required for a whole measurement period is known in a specific application.

To summarize, the proposed charge-based storage estimation method can directly use the manufacturer-provided leakage current to calculate the total charge stored, which entirely avoids the complicated calculation for energy loss during the charge redistribution process. Accordingly, this new method is generic for any IoT application since it is independent of the initial charge state and charge history of the supercapacitors.

III. VALIDATION EXPERIMENTS

The IoT node developed for building air quality control, as shown in Fig. 4, is composed of a PV power supply, a microcontroller, and the wireless link. When a low-power CO_2 gas sensor [19] is adopted to measure CO_2 levels every 150 s, it requires 4.24-mC total discharge (including active and sleep modes) in an entire measurement period [14]. The circuit diagram of the system, which employs a supercapacitor alone as the storage for indoor sub-mW PV energy harvesting power supply to achieve a lifetime battery-replacement-free solution, is shown in Fig. 5. At the recommended lowest indoor illumination level of 200 lx, the open-circuit voltage of the 50 × 20 mm indoor PV panel is 4.6 V, whereas the short-circuit current is 45 μA. The high PV output voltage makes it possible to directly store the PV harvested energy into a supercapacitor using a simple charger, in this case the LTC4071 from Linear Technology. V_H/V_L is the overcharge/overdischarge protection voltage. D_2 is a protection diode to stop the PV panel being charged by the 5.4V 0.5F VinaTech supercapacitor when the illumination condition is poor. R_0 is a charge current limitation resistor to protect the whole charge circuit.

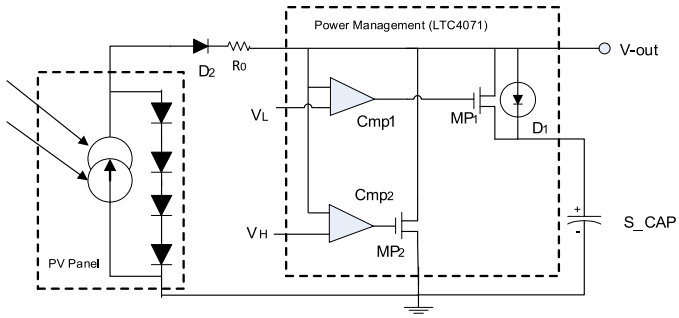

Fig. 5. Supercapacitor employed for energy storage with overcharge and overdischarge protections.

According to the proposed charge-based storage evaluation method, the amount of charge from the PV (at 200 lx) in an entire measurement period can be calculated as 45 μA × 150 s = 6.75 mC, the leaked charge can be calculated as 2 μA × 150 s = 0.3 mC, and the known amount of discharge from the load is 4.24 mC, so the net charge in a measurement period is calculated as 6.75-0.3-4.24 = 2.21 (mC), corresponding to a terminal voltage increase of 2.21 mC/0.5F = 4.42 mV for each measurement period. Experiments carried out to validate the above-mentioned calculation, by recording and analyzing the terminal voltage of the supercapacitor, are described below.

A. Leakage Current Validation

The key point of the newly proposed method is that the leakage current of the supercapacitor in an IoT application is the same as the manufacturer-specified one. To validate this, the circuit shown in Fig. 5 has been attached to a simulated IoT load, as shown in Fig. 6, so that the amount of discharge by the load can be obtained via recording the terminal voltage of the supercapacitor. The simulated load contains two load resistors, $R_1 = 200\Omega$ for active mode, and $R_2 = 1\text{M}\Omega$ for sleep mode. A mode switch connects the supercapacitor to its load; it is controlled to respond at a measurement timing of 250-ms active

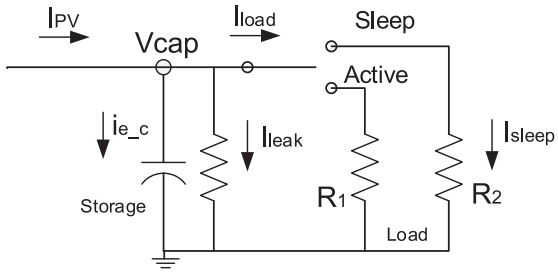

Fig. 6. Simulated resistive load for leakage current validation. With the recorded terminal voltage $V_{\rm cap}$, the supercapacitor discharged by the load in an entire measurement period can be obtained experimentally.

mode in a 150-s total measurement period, corresponding to the timing for practical CO_2 measurements.

The idea of this experiment is that by using the recorded terminal voltage, the amount of discharge ($Q_{\rm dis}$) of the supercapacitor in a measurement period can be expressed as

$$Q_{\rm dis} = \frac{\int_{t_1}^{T_{2-s}} v_{\rm cap}\,(t)\,dt}{R_2} + \frac{\int_{T_{2-s}}^{T_{2-e}} v_{\rm cap}\,(t)\,dt}{R_1} + \frac{\int_{T_{2-e}}^{T-t_1} v_{\rm cap}\,(t)\,dt}{R_2} \quad (4)$$

where t_1 is the measurement start point in sleep period, T_{2-s} and T_{2-e} are, respectively, start and end active modes (T_{2-e}–$T_{2-s} = T_2$).

The amount of charge change ΔQ in a measurement period can be expressed by

$$\Delta Q = C\,(T+t_1)\,v_{\rm cap}\,(T+t_1) - C\,(t_1)\,v_{\rm cap}\,(t_1) \quad (5)$$

where the variation of the capacitance of the supercapacitor $C(t)$ in formula (5) is reflected by terminal voltage change of the supercapacitor. When t_1 in formula (5) is selected in sleep mode, the effective charge current $I_{e-c} = I_{\rm pv} - I_{\rm sleep} - I_{\rm leak}$ (shown in Fig. 6) is a constant, so the capacitance of the supercapacitor can be expressed as

$$C\,(t) = \frac{dQ}{dV_{\rm cap}\,(t)} = \frac{I_{e\_c}dt}{dV_{\rm cap}\,(t)} = \frac{(I_{\rm pv} - I_{\rm sleep} - I_{\rm leak})}{\frac{dV_{\rm cap}\,(t)}{dt}} \quad (6)$$

where $\frac{dV_{\rm cap}\,(t)}{dt}$ is the terminal voltage change with time. If the recorded terminal voltage change of $\frac{dV_{\rm cap}\,(t)}{dt}$ is a constant, $C(t)$ will be a constant so the charge redistribution process should be completed and it holds $C(T+t_1) = C$ and $C(t_1) = C$ (C is the nominal capacitance). Therefore, formula (5) becomes

$$\begin{aligned}\Delta Q &= C\,(T+t_1)\,v_{\rm cap}\,(T+t_1) - C\,(t_1)\,v_{\rm cap}\,(t_1)\\ &= C\,[v_{\rm cap}\,(T+t_1) - v_{\rm cap}\,(t_1)] = C\Delta v_{\rm cap}. \end{aligned} \quad (7)$$

This makes ΔQ an obtainable figure. Combining formulae (1), (4), and (7), the target of experimentally acquiring the leakage current of the supercapacitor in IoT applications can be achieved.

1) Experiment Set-Up: To obtain leakage current in μA accuracy, the recorded terminal voltage of the supercapacitor should be less than $V_{\rm min}\{1.0\ \ \mu{\rm A} \times 200\ \Omega,\ 1\ \mu{\rm A} \times 1\ {\rm M}\Omega\}$ = 0.2 mV. The minimum voltage recording duration Δt has been determined in T_1 as $\Delta t \le 4.5\,{\rm ms}$ from $V = v_0 e^{-\frac{t}{R_2 C}}$, $|\frac{dV}{dt}|\Delta t = \frac{v_0}{R_2 C} e^{-\frac{t}{R_2 C}} \Delta t \le \frac{v_0}{R_2 C}\Delta t \le 0.2\,{\rm mV}$, where V_0 is selected as 4.2 V (the V_H in Fig. 5), R_2 is 200 Ω and C = 0.5 F.

The timing signal of 250 ms for active mode and 149.75 s for sleep mode has been created using a signal generator to control the mode switch in Fig. 6, as well as to trigger the four-channel oscilloscope (MSO9064A), which runs in segmented memory mode to record the required voltage data. The high-resolution mode (12 b) of the oscilloscope is selected. The data recording sample rate is set as 2 KSPS rather than the required 250 SPS (calculated from the minimum 4.5-ms sampling period) allowing data averaging to improve the signal to noise ratio. The indoor PV panel has been illuminated at 200 lx and the PV current is recorded using a Keithley 2450 SourceMeter. Additionally, the trigger signal is recorded as the timing reference.

2) Results: Supercapacitor voltage segments in 45 successive periods are recorded, as shown in Fig. 7(a). Curves from the bottom to the top correspond to period numbers 1 to 45, demonstrating that the energy harvested is larger than that consumed in each period. Each curve start point ($t = 0$) corresponds to the measurement point at 150 ms, just before the end of sleep mode, and the voltage drop observed is due to the internal resistance of the power supply when the mode switch turns ON to active mode. Similarly, a voltage jump is seen when the mode switch turns OFF. Note that the starting voltage of each curve is the voltage at the end of previous charge period. The voltage of each curve at 100 ms has been plotted in Fig. 7(b) as the blue curve (marked with "o"). This shows an increasing voltage after each entire measurement period. The linear relationship implies that the net charge change to the capacitor in every measurement period is almost the same. The PV supplied charge current is shown as the red curve (marked with "□") in Fig. 7(b) as well. The recorded PV current changes are smaller than 0.6 μA within 2 h when the supercapacitor voltage changes from 3.703 to 3.817 V, verifying that PV current during the recording period can be treated as a constant of the mean value of 44.9 μA. Since the employed oscilloscope has an input impedance of 1 MΩ, a leakage path with 1 MΩ resistance in parallel with the supercapacitor in Fig. 6 is included for later leakage current calculation.

The linearity of the terminal voltage [0–350 ms in Fig. 7(a)] was examined, as shown in Fig. 7(c); it shows the voltage difference after 40 consecutive periods to reduce the measurement noise effects, and it demonstrates that before the end of the sleep mode, the voltage change is constant. Since this constant voltage change period is observed before the end of sleep mode, it implies that the supercapacitor is in a steady state with the nominal capacitance. In contrast, the voltage change in active mode [from 150 to 350 ms in Fig. 7(c)] is not constant, indicating a capacitance change period.

The terminal voltage change at before the end of sleep mode has been used for charge calculation. The experimental results and the leakage current calculated using C = 0.5 F at t_1 = 100 ms in Fig. 7(a) are shown in Table II. It shows that the measured average leakage current (1.8 μA) is almost the

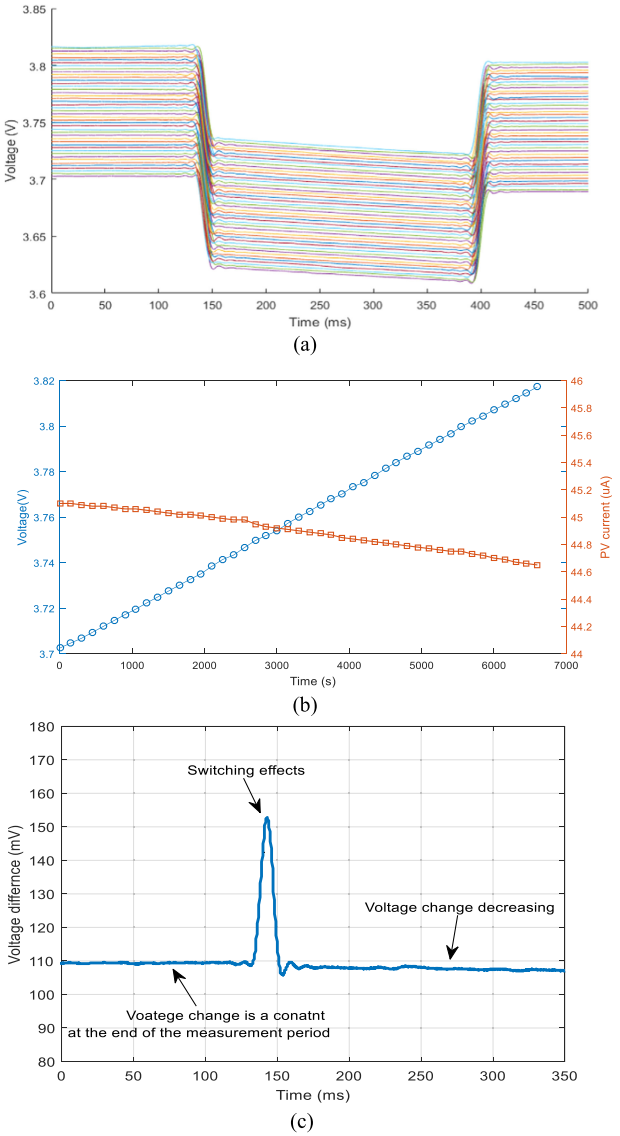

Fig. 7. (a) Measured raw data of the terminal voltage of the supercapacitors in 45 successive periods. (b) Voltages of each period at 100 ms (blue curve) and the output current of the PV energy harvester (red curve). (c) Linearity check.

same as that specified by the manufacturer (2.0 μA). Therefore, the key point of the proposed method, that leakage current of the supercapacitor in IoT applications is the same as the manufacturer-specified one, has been validated experimentally.

A full comparison between the calculated results acquired through the proposed method and the experimentally measured results is listed in Table III. The first measurement period, where the terminal voltage of the supercapacitor is set at 3.703 V and the PV supplied current is 45 μA, has been used for calculations performed in accordance with the proposed method. The I_{load} has been calculated using formula (1), and the ΔV is calculated using $I_{e\_c} \times T = C \times \Delta V$. The calculated terminal voltage increase after a measurement period is 2.54 mV, which represents a 0.4% difference from the average of 2.53 mV calculated using the 45 measurement periods shown in Fig. 7(b) (voltage increased from 3.703 to 3.817 V), demonstrating that

TABLE II
PARAMETER SUMMARY DURING 45 MEASUREMENT PERIODS

Active period (T_1)	250 ms
Sleep period (T_2)	149.75 s
Supercapacitor voltage1 (start)	3.71 V
Supercapacitor voltage2 (stop)	3.82 V
Total charge/I_{pv} from PV	296.3 mC / 44.9μA
Capacitor saved charge/ Ie_c	57 mC / 8.6 μA
Total discharge / I_{load}	224.4 mC / 34.0 μA
Leaked charge/total leakage current	14.9 mC/ 2.3 μA
Typical supercapacitor leakage current	1.8 μA

TABLE III
COMPARISON OF PROPOSED CALCULATION AND EXPERIMENT RESULTS

	Proposed calculation (first period)	Experiment results (average of 45 periods)
PV current	45 μA (specified)	44.9 μA
I_{load}	$\frac{\frac{3.703}{200}\times 149.75+\frac{3.703}{1000000}\times 0.25}{150}$ = 34.5 (μA)	34.0 μA
I_{leak}	2.0 μA (specified)	1.8 μA
I_{e_c}	(45-34.5-2) μA = 8.5 μA	8.6 μA
ΔV	150 s×8.5 μA /0.5 F = 2.54 mV	(3.817-3.703) V/45 = 2.53 mV

the proposed method can be used for charge storage estimation in supercapacitor's IoT applications.

B. Validation Through a Practical IoT Application

CO_2 concentration measurements, using the indoor PV energy harvesting powered autonomous IoT sensor nodes shown in Fig. 4, have been carried out for further validation of the proposed method, since the leakage current of the supercapacitor listed in Table II is a "typical" value obtained by using the maximum quiescent current (0.5 μA) of the power management chip of LTC4017. In this experiment, the terminal voltage increase of the supercapacitor was measured after an entire measurement period so that the supercapacitor leakage current and the quiescent current of the power management chip could be taken into account as a whole.

During the validation, the sensor node was being set in active mode for 250 ms in every 150 s when the indoor PV energy harvester was illuminated at 200 lx. The Keithley DMM7510 multimeter was recording the supercapacitor terminal voltage at 100 ms before the end of sleep mode of each measurement period, as shown in Fig. 8(a). This demonstrated that the terminal voltage of the supercapacitor increased from the precharged 4.099 V to the preset overcharge protection voltage of 4.195 V in 80 measurement periods.

The curve shown in Fig. 8(a) is composed of three parts. In the first 14 measurement periods, the terminal voltage increases almost linearly. This is then followed by a nonlinear voltage increase area until the period 61, and finally the terminal voltage is fixed at 4.195 V during the rest of periods due to the overcharge protection. The average effective charge current for the first 14 periods is calculated as $\frac{C\Delta V}{14T} = 9.76\,\mu$A. When considering that the known total load discharge is 4.24 mC in the 150-s measurement period, corresponding to a discharge current

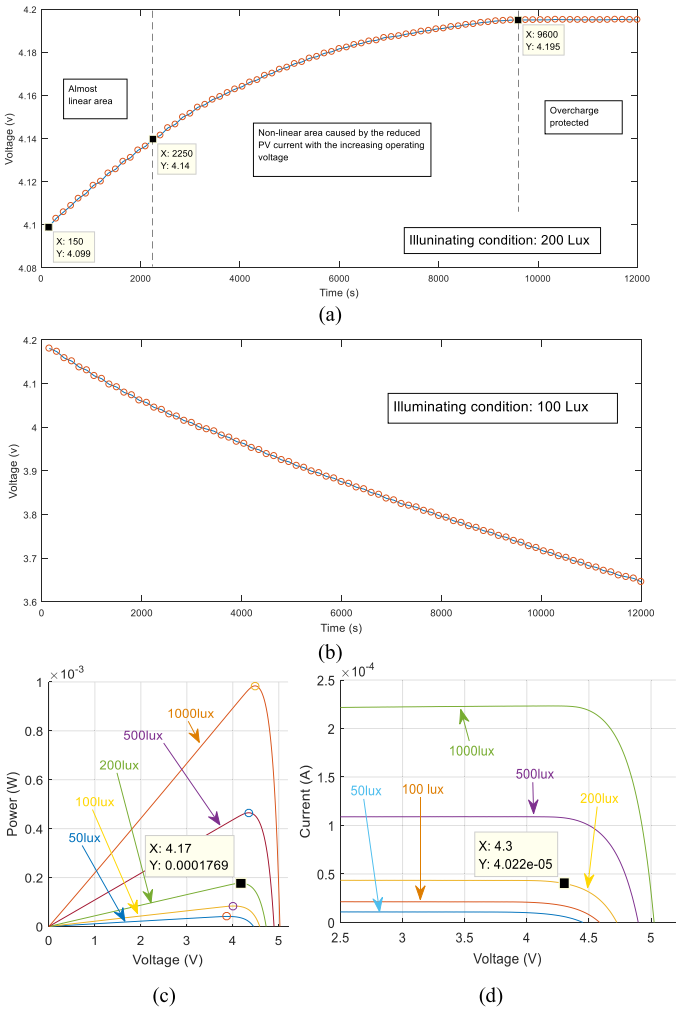

Fig. 8. Terminal voltage of supercapacitor recorded at the end of sleep mode for IoT-based CO_2 measurements. (a) Increasing voltage at 200-lx illumination demonstrates that the charge is larger than the discharge of the supercapacitor in every measurement period. (b) Decreasing voltage at 100-lx illumination demonstrates that the charge is smaller than discharge. (c) Power output of the adopted PV showing a maximum power point of 4.17 V at 200 lx. (d) Measured *I–V* curve showing a reduced PV current when operating voltage is over the maximum power point.

of 28.3 μA, it seems that the experimentally obtained leakage current of the supercapacitor of [45 μA (PV charge current) – 28.3 μA (load consumed current) – 9.76 μA (effective charge current)] = 6.94 μA is much higher than that of manufacturer specified of 2.0 μA. This result seems conflicting to the validated result in Section III-A wherein the leakage current of a supercapacitor in an IoT application is the same as that specified by the manufacturer. The explanation is that in the measured *I–V* curve of the adopted PV panel [shown in Fig. 8(c) and (d)], the constant PV output current [the linear parts shown in Fig. 8(c) and the flat parts shown in Fig. 8(d)] exists only before the operating voltage of the PV reaches its maximum power point. The maximum power point of the adopted PV at 200 lx is 4.17 V, as shown in Fig. 8(c), whereas the averaged supercapacitor voltage in the first 14 periods shown in Fig. 8(a) is 4.1 V. Since there is a 0.2-V voltage drop on the diode (shown in Fig. 5), the actual PV operating voltage in this experiment is 4.3 V (4.1-V supercapacitor voltage plus a 0.2-V diode voltage drop), corresponding to a 40.2 μA PV current, as shown in Fig. 8(d). The actual leakage current of the supercapacitor obtained by this experiment should be updated as [40.2 μA (PV charge current)—28.3 μA (load consumed current)—9.76 μA (effective charge current)] = 2.14 μA (including the quiescent current of LTC4017), which is similar to the total leakage current of 2.3 μA listed in Table II.

Since the PV current at operating voltage of 4.3 V is 40.2 μA, the amount of charge from PV should be updated as [40.2 μA $\times$ 150 s] = 6.03 mC. The calculated voltage increase at the beginning of Section III should be updated as [(6.03–4.24–2.14 $\times$ 0.15) mC/0.5] = 2.94 mV, which is almost the same as the measured average voltage increase in the first 14 periods of (4.14–4.009)V/14 = 2.93 mV ($<$ 0.3% error). The nonlinear terminal voltage increase in Fig. 8(a) can be explained by the gradual decrease in PV current with the gradually increasing operating voltage of the PV, as shown in Fig. 8(d), when the operating voltage of the PV is over the maximum power point. Repeating the experiment at the illuminating condition of 100 lx, the terminal voltage of the supercapacitor decreases, as shown in Fig. 8(b). According to the proposed method, the amount of charge that the PV provided in a measurement period at 100 lx (22.5 μA PV current) is calculated as 22.5 μA $\times$ 150 s = 3.875 mC, which is already less than the load discharge of 4.24 mC. As a consequence, the terminal voltage of the supercapacitor keeps decreasing in each measurement period. It should also be noted that the discharge rate in Fig. 8(b) decreases at the beginning and then it is almost constant after the terminal voltage becomes lower than 4.0 V, which can be explained when considering the maximum power point of 4.0 V at 100 lx, as shown in Fig. 8(c).

In summary, the experimental results shown in Fig. 8(a) and (b) demonstrate that the supercapacitor storage can be accurately predicted by the newly proposed method, therefore, the proposed method can be directly used for calculation of the storage capacity of a supercapacitor for IoT applications.

It is worth noting that the quiescent current of a commercially available power management chip is reported as 325 nA [20] and the developed application system using this chip (such as Bluetooth Low Power beacon [21]) seems to have already provided a solution for indoor PV-powered applications. However, when the illumination goes down to 250 lx, the reported PV-harvested power of ~200 μW cannot charge the adopted supercapacitor when the load power consumption is set as 180 μW, even without considering the power consumption contributed by the leakage current of the supercapacitor. The reported operating illumination is 450 lx corresponding to an almost doubled harvesting power while the load is still set as 180 μW. Since no quantitate calculation exists, it is reasonable to assume that 450 lx is the lowest usable operating illumination, suggesting that the reported power management solution cannot be utilized for sub-mW indoor PV energy harvesting. In contrast, the charge-based method reported in this paper can provide a feasible solution by direct calculation. The leakage current of the adopted supercapacitor is specified as 2.0 μA and the specified maximum current consumption of the charge management chip is 0.5 μA. When

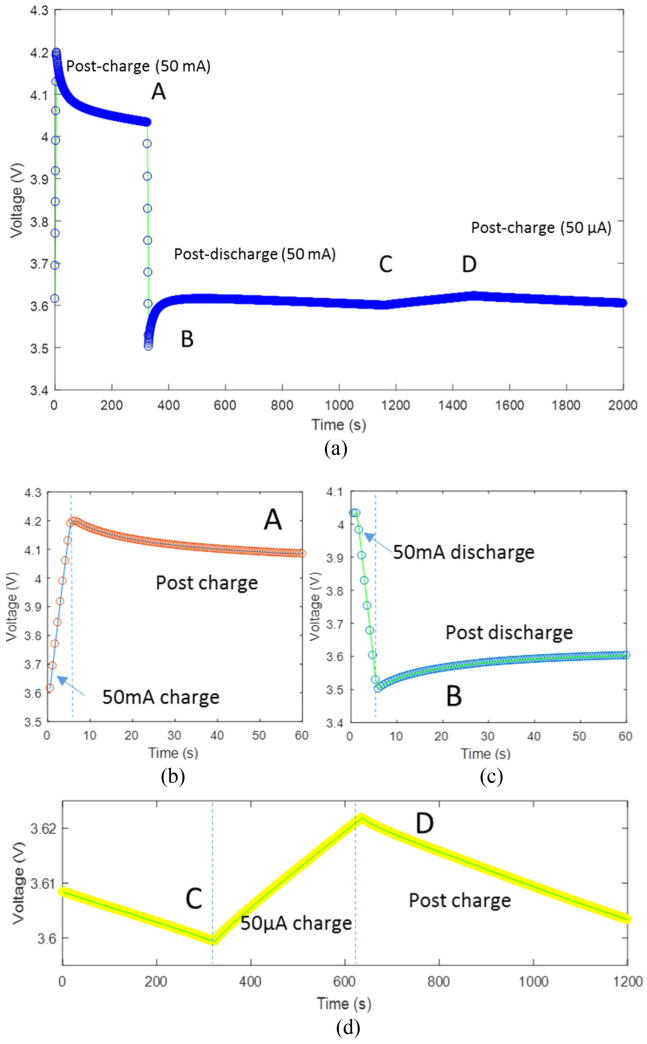

Fig. 9. (a). Recorded terminal voltage of a 0.5F supercapacitor. Charge redistribution caused voltage changes can be observed at A [postcharge of 50 mA shown in (b)] and B [postdischarge of 50 mA shown in (c)]. No charge redistribution can be observed at D [postcharge of 50 μA beginning at C shown in (d)].

the operating voltage of the system is set as 4.0 V, the supercapacitor and the adopted simple charger chip consume a total power of 10 μW; therefore, after powering the required 180 μW, there is still 10 μW left for charging the supercapacitor. In fact, when the ultra-low-power power management chip reported in [20] is connected to the indoor PV panel, adopted in this paper, at 200 lx (180-μW harvested power), the observed terminal voltage of the supercapacitor decreased even when there is no load applied, indicating that the supercapacitor is not charged at all.

C. Discussion

When a 0.5-F supercapacitor is charged at 50 mA current and then discharged at 50 mA current after 5 min, the recorded terminal voltage changes, as shown in Fig. 9(a) (case A and case B). This clearly demonstrates the two charge redistribution processes that consume energy. In case A shown in Fig. 9(b), an exponential drop in the terminal voltage of 100 mV can be observed after 60 s of charge. Similarly, in case B shown in Fig. 9(c), an exponential voltage rise can be observed. The supercapacitor is charged again at point C at 50 μA current and charging is stopped at point D shown in Fig. 9(d). The almost linear terminal voltage curve around C and D demonstrates that there is minute charge redistribution process. In practice, at least one charge redistribution process can be observed at the end of active mode in sub-mW indoor PV-powered IoT applications.

Charge redistribution incurred energy loss can be high. When considering that the energy loss of the charge redistribution between two identical capacitors can be as high as 50% when the initial charge condition is set as one fully charged and the other empty in charge, energy loss of the charge redistribution process must be taken into account for energy-based storage evaluation. Referring to Fig. 2, energy loss in charge redistribution process can be obtained using formula (2) as

$$E_{\text{loss}} = \int_0^{n\tau} i_1^2(t)\, R_1\, dt = \int_0^{n\tau} \left(\frac{(V_0 - V_1)^2}{R_1} e^{-\frac{2t}{\tau}} \right) dt$$
$$= \frac{(V_0 - V_1)^2}{R_1} \int_0^{n\tau} \left(e^{-\frac{2t}{\tau}} \right) dt \tag{8}$$

where $\tau = R_1 \frac{C_0 C_1}{C_0 + C_1}$ and n = 3–5, V_0 and V_1 are the initial voltages of the charge redistribution. The term $\int_0^{n\tau} (e^{-\frac{2t}{\tau}}) dt$ is constant for a given model after the completion of charge redistribution, so the energy loss is mainly determined by $(V_0 - V_1)$. If the initial charge state parameters of V_1 and V_0 are known, energy loss can be easily calculated, as reported in [9]. In practical applications, $(V_0 - V_1)$ is usually unavailable. Even with a known charge current, $(V_0 - V_1)$ cannot be obtained, since when referring to Fig. 3, the initial charge state parameters of V_1 and V_0 in formula (8) are determined by the charge process as

$$\begin{cases} \dfrac{C_0 V_0}{i_0} = \dfrac{C_1 V_1}{i_1} \\ I_{\text{charge}} = i_0 + i_1 \end{cases} \tag{9}$$

where i_0 and i_1 denote the currents flowing through capacitance C_0 and C_1. Formula (9) has three unknown parameters in two equations so it has infinite solutions, making simulation the only possible way for energy-based storage evaluation.

In contrast, the charge-based storage estimation method analyzes the circuit in current mode [22] using the amount of charge calculated by $I \times t$, which is more suitable for the PV-powered applications, where PV cell is modeled as a current source. The proposed charge-based storage estimation treats the supercapacitor as a black-box to calculate the charge stored inside the supercapacitor through terminal current input/output. Since the manufacturer-provided leakage current has been linked to the supercapacitor model in Section II-B, no experiment is required to obtain the supercapacitor's model parameters and no simulation is required for the dynamically changing charge redistribution current.

It seems that using energy-based storage evaluation is a straightforward way for energy harvesting applications.

TABLE IV
STORAGE EVALUATION: ENERGY VERSUS CHARGE

	Reported energy-based methods [4, 9, 10,11]	This work (charge-based)
Model working mode	Voltage	Current
Estimation terms and their linearity	Energy (½CV², $i_1^2R_1t$) Non-linear	Charge (I×t, CV) linear
Model parameters required	Yes (A set of R and C gained by further experiment)	No (Manufacture already provided)
Initial condition	Required	Not required
Estimation method	Full simulation	Direct calculation
Expt. validated	No	Yes
Practical to use	No	Yes

However, using charge domain can make the case easier since, while energy is expressed by $I \times t \times V$, charge is expressed as $I \times t$, where V is the terminal voltage of the supercapacitor that changes nonlinearly due to the charge redistribution process. Also when estimating storage via energy, the calculation terms used are ½CV², $i_1^2 R_1 t$, whereas the terms used in charge evaluation are $I \times t$ and $C \times V$, so the proposed charge-based method directly uses formulas for calculation, whereas the energy-based method relies on simulations. This is supported by the fact that the charge-based method has been experimentally validated by simple recording and analysis of the terminal voltage of the supercapacitor, whereas validation of energy-based methods (as presented in the literature) has not been reported yet. A full comparison of the charge and energy-based storage evaluation methods is listed in Table IV.

Analysis of a PV energy harvesting powered IoT node in the newly proposed current mode also helps to explain the reason why there is almost no charge redistribution after the end of sleep mode. Referring to Fig. 6, the net charge current in sleep mode is $I_{e\_c} = (I_{\rm pv} - I_{\rm leak} - I_{\rm sleep})$, so when using formula (9), the maximum current flow through the C_1 branch in Fig. 3 is calculated as

$$I_1 = \frac{C_1 V_1}{C_0 V_0 + C_1 V_1} \times I_{e\_c} = \frac{C_1}{C_0 \frac{V_0}{V_1} + C_1} \times I_{e\_c} < \frac{C_1}{C_0 + C_1} \times I_{e\_c} \quad (10)$$

due to $V_1 = V_0 - I_1 R_1 < V_0$. When using model parameters of [9] listed in Table I ($R_1 = 100\ \Omega$, $C_0 = 8.44$ F and $C_1 = 3.44$ F) and $I_{e_c} = (45 - 2 - 4) = 39\tilde{}\mu$A, the current I_1 is calculated as 11.2 μA resulting in a 1.12 mV voltage difference between C_0 and C_1. This tiny voltage difference corresponds to a maximum instant power loss of 12.67 nW at the beginning of the charge redistribution process and therefore the charge redistribution process is negligible in terms of storage energy loss. Similarly, when a 50 mA current is drawn from the supercapacitor in active mode, I_1 is calculated as less than 14.3 mA producing a <1.43 V voltage difference between C_0 and C_1 after the end of active mode. This large voltage difference results in 20.6 mW maximum instant power loss at the beginning of charge redistribution and therefore there is a considerable charge redistribution process at the end of active mode when energy loss is considered.

TABLE V
LEAKAGE CURRENT COMPARISON OF LI-BATTERY AND SUPERCAPACITOR

	Supercap (5.4 V 0.5 F)	Li-Battery (CP 1254 50 mAH)
Specified leakage current (μA)	2.0	N/A
Measured leakage current (μA)	2.0	1.0 [25]
Percentage (leakage/PV current)	4.4%	2.2%

The estimated 1.43 V voltage difference is relatively high when considering that the voltage output is about 4.0 V. In practice, since the discharge time period in IoT applications is very limited (in the hundred ms range), even in the case of 1-s active period discharged at $I = 50$ mA, the voltage difference is limited to 5.89 mV due to the small amount of discharge ($\Delta V < \frac{I\Delta t}{C_0}$). Therefore, terminal voltage drop caused by charge redistribution is not an issue for IoT applications when considering that the total amount of discharge is relatively small when compared with the total charge stored in the supercapacitor.

It is also worth noting that the 2.0 μA leakage current of the 5.4-V 0.5-F supercapacitor is low even when compared with the ultralow leakage current of 1.0 μA [23] measured from a coin Lithium battery of CP 1254 from Varta Microbattery GmbH. Therefore, as shown in Table V, the leakage current of the supercapacitor is not an issue in indoor sub-mW PV energy harvesting applications when comparing it with the PV current of 45 μA at 200 lx. It should also be highlighted that the leakage current of the 5.4-V 1.0-F supercapacitor from the same manufacturer is specified as 4.0 μA, therefore, the leakage current of the supercapacitor is proportional to the storage capacity. If a 10-F supercapacitor was adopted for a larger storage capacity, the estimated 40 μA leakage current would not be acceptable for the applications reported in this paper.

IV. CONCLUSION

Self-discharge has been the key concern preventing supercapacitors from being used as the sole storage component in sub-mW indoor PV energy harvesting powered IoT applications for lifetime battery-replacement-free solutions, because of the difficulty in evaluating the energy loss in the charge redistribution process, which occurs in every measurement period for IoT applications.

The proposed storage evaluation method provided a new view of calculating the total amount of charge stored in current mode, using $I \times t$, successfully avoiding using the dynamically changing parameters of C and V for storage evaluation in the charge redistribution process. Time constant analysis and leakage current test experiments demonstrated that the manufacturer-specified tiny leakage current, although measured several days after charge, could be directly used in the charge-based storage evaluation, making the proposed method straightforward without further requirements for acquiring model parameters of the supercapacitor or for determining the initial charge state.

Finally, the tiny leakage current of the supercapacitor at the required storage capacity for sub-mW indoor PV energy harvesting applications, as revealed by the proposed method, strongly supported that a supercapacitor could be the sole storage element for PV-powered IoT nodes. Consequently, a solution is provided for lifetime battery-replacement-free applications.

REFERENCES

[1] A. Al-Fuqaha, M. Guizani, M. Mohammadi, M. Aledhari, and M. Ayyash, "Internet of things: A survey on enabling technologies, protocols, and applications," *IEEE Commun. Surv. Tutorials*, vol. 17, no. 4, pp. 2347–2376, Oct./Dec. 2015.

[2] F. Simjee and P. Chou, "Efficient charging of supercapacitors for extended lifetime of wireless sensor nodes," *IEEE Trans. Power Electron.*, vol. 23, no. 3, pp. 1526–1533, May 2008.

[3] M. Uno and K. Tanaka, "Accelerated charge–discharge cycling test and cycle life prediction model for supercapacitors in alternative battery applications," *IEEE Trans. Ind. Electron.*, vol. 59, no. 12, pp. 4704–4712, Dec. 2012.

[4] H. Yang and Y. Zhang, "Analysis of supercapacitor energy loss for power management in environmentally powered wireless sensor nodes," *IEEE Trans. Power Electron.*, vol. 28, no. 11, pp. 5391–5403, Nov. 2013.

[5] T. J. Freeborn, B. Maundy, and A. S. Elwakil, "Measurement of supercapacitor fractional-order model parameters from voltage-excited step response," *IEEE J. Emerg. Sel. Topics Circuits Syst.*, vol. 3, no. 3, pp. 367–376, Sep. 2013.

[6] R. German, A. Hammar, R. Lallemand, A. Sari, and P. Venet, "Novel experimental identification method for a supercapacitor multipore model in order to monitor the state of health," *IEEE Trans. Power Electron.*, vol. 31, no. 1, pp. 548–559, Jan. 2016.

[7] M. Kaus, J. Kowal, and D. Sauer, "Modelling the effects of charge redistribution during self-discharge of supercapacitors," *Electrochimica Acta*, vol. 55, pp. 7516–7523, 2010.

[8] V. Sedlakova *et al.*, "Supercapacitor equivalent electrical circuit model based on charge redistribution," *J. Power Sources*, vol. 286, pp. 58–65, 2015.

[9] R. Chai and Y. Zhang, "A practical supercapacitor model for power management in wireless sensor nodes," *IEEE Trans. Power Electron.*, vol. 30, no. 12, pp. 6720–6730, Dec. 2015.

[10] Y. Diab, P. Venet ; H. Gualous, and G. Rojat, "Self–discharge characterization and modelling of electrochemical capacitor used for power electronics applications," *IEEE Trans. Power Electron.*, vol. 24, no. 2, pp. 510–517, Feb. 2009.

[11] A. Nasiri, S. Zabalawi, and G. Mandic, "Indoor power harvesting using photovoltaic cells for low-power applications," *IEEE Trans. Ind. Electron.*, vol. 56, no. 11, pp. 4502–4509, Nov. 2009.

[12] W. Wang *et al.*, "Design considerations of sub-mW indoor light energy harvesting for wireless sensor systems," *ACM J. Emerg. Technol. Comput. Syst.*, vol. 6 no. 2, 2010, Art. no. 6

[13] Y. Wang *et al.*, "Storage-less and converter-less photovoltaic energy harvesting with maximum power point tracking for internet of things," *IEEE Trans. Comput.-Aided Des. Integr. Circuits Syst.*, vol. 35, no. 2, pp. 173–186, Feb. 2016.

[14] X. Yue *et al.*, "Development of an indoor photovoltaic energy harvesting module for autonomous sensors in building air quality applications," *IEEE Internet Things J.*, vol. 4, no. 7, pp. 2092–2103, Dec. 2017.

[15] X. Yue, J. Kiely, A. Farooq, and A. Champneys, "Estimation of the dynamic leakage current of a supercapacitor in energy harvesting powered autonomous wireless sensor nodes," in *Proc. IEEE Int. Telecommun. Energy Conf.*, 2017, pp. 278–281

[16] A. Lewandowski, P. Jakobczyk, M. Galinskia, and M. Biegun, "Self-discharge of electrochemical double layer capacitors," *Phys. Chem. Chem. Phys.*, vol. 15, pp. 8692–8699, 2013.

[17] A. S. Weddell, G. V. Merrett, T. J. Kazmierski, and B. M. Al-Hashimi, "Accurate supercapacitor modeling for energy harvesting wireless sensor nodes," *IEEE Trans. Circuits Syst.-II, Express Briefs*, vol. 58, no. 12, pp. 911–915, Dec. 2011.

[18] Y. Zhang and H. Yang, "Modelling and characterization of supercapacitors for wireless sensor network applications," *J. Power Sources*, vol. 196, pp. 4128–4135, 2011.

[19] D. Gibson and C. MacGregor, "A novel solid state nondispersive infrared CO_2 gas sensor compatible with wireless and portable deployment," *Sensors*, vol. 13, pp. 7079–7103, 2013.

[20] S. Kim *et al.*, "Ambient RF energy-harvesting technologies for self-sustainable wireless sensor platforms," *Proc. IEEE*, vol. 102, no. 11, pp. 1649–1666, 2014.

[21] Texas Instrum., Dallas, TX, USA, "Indoor light energy harvesting reference design for Bluetooth Low Energy (BLE) beacon subsystem," 2014. [Online]. Available: http://www.ti.com/lit/ug/tidu235a/tidu235a.pdf

[22] J. Mahattanakul and C. Toumazou, "Current-mode versus voltage-mode $G_m - C$ biquad filters: What the theory says," *IEEE Trans. Circuits Syst.-II, Analog Digit.*, vol. 45, no. 2, pp. 173–186, Feb. 1998.

[23] X. Yue *et al.*, "A successive approximation method to precisely measure leakage current of the rechargeable Lithium coin battery," *J. Energy Storage*, vol. 13, pp. 442–446, 2017.

Xicai (Alex) Yue (M'14–SM'15) received the B.Eng. degree in telecommunication engineering, and the M.Eng. and Ph.D. degrees in biomedical engineering from Xi'an Jiaotong University, Xi'an, China, in 1985, 1995, and 1999, respectively.

He was a University Teaching Assistant and then a Lecturer in digital switching in China after graduation. From 1999 to 2016, he was with Tsinghua University, Beijing, China, Imperial College London, London, U.K., and Sharp Laboratories of Europe, Oxford, U.K. He is currently a Senior Lecturer and the Head of instrumentation with the Institute of Bio-Sensing Technology, University of the West of England, Bristol, U.K. He has authored or coauthored more than 20 peer-reviewed journal papers (as lead author) and a book chapter. His current research interests include active dry-electrodes for physiological measurements, low-power mixed-signal CMOS IC design for biomedical and wearable bio-sensing applications.

Dr. Yue is an Associate Editor for the Elsevier's *Measurement* journal. He was a recipient of the Live Demo Special Session Award of the IEEE International Symposium on Circuits and Systems in 2007.

Janice Kiely received the B.Eng.(Hons.) degree in electronic engineering from the University of Sheffield, Sheffield, U.K., in 1987, and the Ph.D. degree from the University of Cardiff, Cardiff, U.K., in 1992. Her Ph.D. involved the development of novel, miniature thermoelectric devices for passive IR detection.

She was appointed as a Lecturer in Sensors and Instrumentation in 1993 and subsequently has held the roles of the Head of the Department of Electronic and Computer Systems Engineering and the Head of Research and Knowledge Exchange for the Faculty of Engineering. Since 2008, she has been the Co-Director of the Institute of Bio-Sensing Technology, Bristol, U.K., and since 2016, the Health Technology Hub, University of the West of England, Bristol, U.K. In 2014, she was the Founder of a University spin out, MIAtech Biosolutions, Ltd.

Prof. Kiely is a Fellow of the Institute of Engineering and Technology, U.K., and in 2015 she was awarded a Royal Academy of Engineering Enterprise Fellowship.

Des Gibson received the B.Sc.(Hons.) degree in pure and applied physics and the Ph.D. degree in thin film optics from Queen's University Belfast, Belfast, U.K., in 1979 and 1983, respectively.

He has more than 30 years' track record in industry, gained globally with technical and managing director roles within blue chip organizations, small to medium sized companies, start-ups, and close associations with academia. He cofounded four successful physics-based technology companies, focusing on optical thin film and sensor technologies. Two most recent are: Gas Sensing Solutions, Ltd., Cumbernauld, U.K.,—cofounded in 2006 and a recent winner of both Institute of Physics Innovation and Shell Springboard awards—and Applied Multilayers, Ltd., Battle Ground, WA, USA, cofounded in 2002, acquired 2010 by Telemark, Inc., Battle Ground, WA, USA. Motivated by fresh challenges and a desire to focus on research, in 2014 he joined the University of the West of Scotland (UWS) as a Professor in Thin Film and Sensor Technologies and is the Director and Founder of the Institute of Thin Films, Sensors and Imaging (www.itfsi.com). He is a named inventor on 17 patents and in 2018 founded a UWS spinout company Albasense, Ltd.

Prof. Gibson is a Fellow of the Institute of Engineering and Technology and the Institute of Physics, and is a Chartered Engineer.

Emmanuel M. Drakakis (M'05) received the four-year B.S. degree in physics and the two-year M.Phil. degree in electronic physics and radioelectrology from Aristotle University of Thessaloniki, Macedonia, Greece, in 1991 and 1994, respectively, and the Ph.D. degree in analog IC design from the Imperial College, London, U.K., in 2000.

He is currently a Professor in bio-circuits and systems with the Department of Bioengineering, Imperial College London. In this department, he founded the Bioinspired VLSI Circuits and Systems Group. He has authored or coauthored a large number of peer-reviewed papers and several book chapters.

Prof. Drakakis is the recipient of many prizes for research excellence and is involved in several cross-disciplinary research projects. He is currently an Associate Editor for the IEEE TRANSACTIONS ON BIOMEDICAL CIRCUITS AND SYSTEMS (2007–present) and *Frontiers in Neuromorphic Engineering*. He is also an Editor for *Measurement*-Elsevier and an Editorial Advisor for BMC *Biomedical Engineering*, Springer *Nature*. He has a cumulative editorial service to the research community of more than 27 years.